DATA-DRIVEN ASSESSMENT OF POST-EARTHQUAKE BRIDGE FUNCTIONALITY AND REGIONAL MOBILITY

FINAL PROJECT REPORT

by

Christopher J. Motter and Adam R. Phillips (Washington State University)
Marc Eberhard, Jeffrey Berman, Brett Maurer (University of Washington)

Sponsorship
PacTrans, WSDOT, Washington State University, University of Washington

for

Pacific Northwest Transportation Consortium (PacTrans)
USDOT University Transportation Center for Federal Region 10
University of Washington
More Hall 112, Box 352700
Seattle, WA 98195-2700

In cooperation with U.S. Department of Transportation,
Office of the Assistant Secretary for Research and Technology (OST-R)

DISCLAIMER

TECHNICAL REPORT DOCUMENTATION PAGE

1. Report No.	2. Government Accession No.	3. Recipient's Catalog No.

4. Title and Subtitle	5. Report Date
Data-Driven Assessment of Post-Earthquake Bridge Functionality and Regional Mobility	February 2023
	6. Performing Organization Code
7. Author(s) and Affiliations	**8. Performing Organization Report No.**
Christopher J. Motter; 0000-0003-0418-3791; and Adam R. Phillips; 0000-0003-2486-6039 – Washington State University Marc Eberhard, Jeffrey Berman, and Brett Maurer; 0000-0001-9305-5745 – University of Washington	2020-M-WSU-3
9. Performing Organization Name and Address	**10. Work Unit No. (TRAIS)**
PacTrans Pacific Northwest Transportation Consortium University Transportation Center for Federal Region 10 University of Washington More Hall 112 Seattle, WA 98195-2700	**11. Contract or Grant No.** 69A3551747110
12. Sponsoring Organization Name and Address	**13. Type of Report and Period Covered**
United States Department of Transportation Research and Innovative Technology Administration 1200 New Jersey Avenue, SE Washington, DC 20590	Final Report, August 2020 – February 2023 **14. Sponsoring Agency Code**

15. Supplementary Notes

Report uploaded to: www.pactrans.org

16. Abstract

The seismic performance of bridges is essential to post-earthquake mobility, as bridges are relied upon to carry goods and people into and out of urban centers after natural disasters. A 2019 Department of Homeland Security (DHS) report assessing the regional resiliency of Western Washington state to a Cascadia Subduction Zone (CSZ) earthquake predicted widespread and high levels of bridge damage. A primary objective of this study was to create an improved prediction of non-functional, partially functional, and functional bridges that will assist in post-earthquake emergency planning. The Washington State Department of Transportation (WSDOT) bridge database was expanded to include site class, properties of abutments and foundations, and additional bridges. Properties of bridges in the database were used to define the parameters for a parametric study on Western Washington bridges subjected to Magnitude 9.0 CSZ ground motions. Detailed multi-degree-of-freedom bridge models were developed with OpenSees. Models were formulated for a suite of representative bridges and used to conduct nonlinear time history analyses for synthetic ground motions that had been generated in previous studies. Results from the model analyses were used to provide a more detailed understanding of the likelihood of bridge damage and the likely service levels post-earthquake. Bridge response was limited in the longitudinal direction because of stiffness provided by the abutments and backfill soil. In the transverse direction, shear keys and bearings were found to limit the lateral deformation in columns as a result of participation of the bridge deck. The majority of bridges in the WSDOT inventory have shear keys and bearings and were predicted to be in full service following a CSZ earthquake. WSDOT has been retrofitting older bridge columns with steel jackets since 1991, and this retrofit has been shown to enhance ductility. Bridges without shear keys and bearings should be prioritized for retrofit. Shorter period bridges near the coast and longer period bridges in locations with sedimentary basins were also identified as being more prone to damage. Bridge functionality after a CSZ earthquake is likely to be considerably better than anticipated by the 2019 DHS report. Some bridges may require repair, but bridges are likely to remain useable for emergency vehicles and post-earthquake response. These conclusions were reached within the scope of the study, with several limitations noted in the report that will require further investigation.

17. Key Words	18. Distribution Statement
Loss; damage; bridge; retrofit; earthquake; Cascadia Subduction Zone	

19. Security Classification (of this report)	20. Security Classification (of this page)	21. No. of Pages	22. Price
Unclassified.	Unclassified.	45	N/A

Form DOT F 1700.7 (8-72) **Reproduction of completed page authorized.**

SI* (MODERN METRIC) CONVERSION FACTORS

APPROXIMATE CONVERSIONS TO SI UNITS				
Symbol	**When You Know**	**Multiply By**	**To Find**	**Symbol**
		LENGTH		
in	inches	25.4	millimeters	mm
ft	feet	0.305	meters	m
yd	yards	0.914	meters	m
mi	miles	1.61	kilometers	km
		AREA		
in^2	square inches	645.2	square millimeters	mm^2
ft^2	square feet	0.093	square meters	m^2
yd^2	square yard	0.836	square meters	m^2
ac	acres	0.405	hectares	ha
mi^2	square miles	2.59	square kilometers	km^2
		VOLUME		
fl oz	fluid ounces	29.57	milliliters	mL
gal	gallons	3.785	liters	L
ft^3	cubic feet	0.028	cubic meters	m^3
yd^3	cubic yards	0.765	cubic meters	m^3
		NOTE: volumes greater than 1000 L shall be shown in m^3		
		MASS		
oz	ounces	28.35	grams	g
lb	pounds	0.454	kilograms	kg
T	short tons (2000 lb)	0.907	megagrams (or "metric ton")	Mg (or "t")
		TEMPERATURE (exact degrees)		
°F	Fahrenheit	5 (F-32)/9 or (F-32)/1.8	Celsius	°C
		ILLUMINATION		
fc	foot-candles	10.76	lux	lx
fl	foot-Lamberts	3.426	candela/m^2	cd/m^2
		FORCE and PRESSURE or STRESS		
lbf	poundforce	4.45	newtons	N
lbf/in^2	poundforce per square inch	6.89	kilopascals	kPa

APPROXIMATE CONVERSIONS FROM SI UNITS				
Symbol	**When You Know**	**Multiply By**	**To Find**	**Symbol**
		LENGTH		
mm	millimeters	0.039	inches	in
m	meters	3.28	feet	ft
m	meters	1.09	yards	yd
km	kilometers	0.621	miles	mi
		AREA		
mm^2	square millimeters	0.0016	square inches	in^2
m^2	square meters	10.764	square feet	ft^2
m^2	square meters	1.195	square yards	yd^2
ha	hectares	2.47	acres	ac
km^2	square kilometers	0.386	square miles	mi^2
		VOLUME		
mL	milliliters	0.034	fluid ounces	fl oz
L	liters	0.264	gallons	gal
m^3	cubic meters	35.314	cubic feet	ft^3
m^3	cubic meters	1.307	cubic yards	yd^3
		MASS		
g	grams	0.035	ounces	oz
kg	kilograms	2.202	pounds	lb
Mg (or "t")	megagrams (or "metric ton")	1.103	short tons (2000 lb)	T
		TEMPERATURE (exact degrees)		
°C	Celsius	1.8C+32	Fahrenheit	°F
		ILLUMINATION		
lx	lux	0.0929	foot-candles	fc
cd/m^2	candela/m^2	0.2919	foot-Lamberts	fl
		FORCE and PRESSURE or STRESS		
N	newtons	0.225	poundforce	lbf
kPa	kilopascals	0.145	poundforce per square inch	lbf/in^2

*SI is the symbol for the International System of Units. Appropriate rounding should be made to comply with Section 4 of ASTM E380.
(Revised March 2003)

TABLE OF CONTENTS

LIST OF FIGURES

LIST OF TABLES

ACKNOWLEDGMENTS

This research was supported by funding from the Pacific Northwest Transportation Consortium (PacTrans) with matching funding provided by the Washington State Department of Transportation (WSDOT), Washington State University, and University of Washington. The authors express their gratitude to PacTrans, WSDOT, Washington State University, and the University of Washington. Any opinions, findings, and conclusions expressed in this material are those of the authors and do not necessarily reflect those of PacTrans, WSDOT, Washington State University, and University of Washington.

The authors would like to acknowledge the valuable contributions and collaboration of Nasser Marafi at Risk Management Solutions for input on the analysis methods of this project. The research presented here builds upon initial analyses performed by the research team on funded WSDOT and US FHWA PacTrans University Transportation Center projects.

Additionally, the authors would like to thank the graduate students who assisted in parts of the modeling or analysis efforts, including Zachary Kortum and Kan-Jen Liu at the University of Washington and Stacia Bell and Sean McGuiness at Washington State University. Thanks are extended to WSDOT engineers Amy Leland, Chase Weeks, Geoff Sweet, and Bijan Khaleghi for providing valuable assistance in access to the WSDOT database and advice on current and historical WSDOT bridge design practices.

EXECUTIVE SUMMARY

The seismic performance of bridges is essential to the post-earthquake mobility of nearly all transportation modes, as bridges are relied upon to carry goods and people into and out of urban centers after natural disasters. Recent research has discovered that the Cascadia Subduction Zone (CSZ), which lies off the western coast of Washington, Oregon, and Alaska, has the potential to generate a Magnitude 9.0 earthquake. The behavior of bridges in Western Washington in a Magnitude 9.0 Cascadia Subduction Zone earthquake was assessed in this study. A Department of Homeland Security (DHS) study (DHS, 2019) attempted to assess the functionality of bridges in Western Washington following a Magnitude 9.0 CSZ earthquake and predicted that approximately 80 percent of the bridges in Western Washington would be unavailable. However, the methods used to generate those predictions were overly crude, making those estimates unreliable. A primary objective of the study summarized in this report was to conduct more refined analyses that could be used to provide more accurate predictions of bridge functionality.

Research Process

The functionality of bridges across Western Washington was estimated as follows:

- The Washington State Department of Transportation (WSDOT) bridge database was expanded to add the properties of 58 additional bridges located on secondary routes that feed into the I-5/405/90 lifeline. These bridges were primarily located west of I-5, with the majority on the Olympic Peninsula. In addition to the added bridges, the WSDOT bridge database was expanded to include properties on abutments and foundations, and the site class for each bridge was identified.
- Properties of bridges in the database were used to define the parameters for a parametric study on Western Washington bridges subjected to Magnitude 9.0 CSZ ground motions. Detailed multi-degree-of-freedom bridge models were developed using OpenSees. The models included abutments, foundations, soil stiffness, and the influence of shear keys between girders, when present. Models were formulated for a suite of representative bridges.
- Nonlinear time history analyses were conducted using the suite of models. Simulated ground motions were used, and these were obtained from previous studies in which 30 scenarios of CSZ earthquakes at ten locations across Western Washington were

simulated. Results from the model analyses were used to provide a more detailed understanding of the likelihood of bridge damage and the likely service levels post-earthquake.

Conclusions

Within the scope of the study, the following conclusions were made, which WSDOT and Washington State emergency planning officials can use to better prepare for a possible Magnitude 9.0 CSZ earthquake:

- The response of the bridges was considerably different in the longitudinal and transverse directions. In the longitudinal direction, the response was limited because of the presence of the abutment and backfill soil, which provided sufficient stiffness to limit the motions. Single-degree-of-freedom models that neglect the effects of the stiffness provided by the abutments and backfill (e.g., models that include only the column stiffness) are likely to result in significant over-prediction of bridge deflections in the longitudinal direction.
- In the transverse direction, the influence of shear keys and bearings on bridge response was significant. Bearings reflect a continuous bridge deck, and shear keys allow the columns to engage with the bridge deck so that the bridge deck provides stiffness in the transverse direction by going into bending. The stiffness provided by the bridge deck was found to significantly limit lateral deformation in the columns.
- For bridges with shear keys and bearings, the median and 85th percentile bent drift ratios were less than the threshold identified for concrete spalling for all bridges considered in the parametric study. Bridges in the WSDOT inventory with shear keys and bearings were predicted to be in full service following a CSZ earthquake. The majority of the bridges in the WSDOT inventory have shear keys and bearings.
- WSDOT has been retrofitting older reinforced concrete bridge columns since 1991. Bridges with retrofitted columns were predicted to be in full service following a CSZ earthquake. This conclusion was based on previous research that showed a low likelihood of failure for these columns.
- Bridges without shear keys and bearings should be prioritized for retrofit. Shorter period bridges near the coast and longer period bridges in locations with sedimentary

basins, such as Seattle and Port Angeles, were identified as being more prone to damage.

- Bridge functionality after a CSZ earthquake is likely to be considerably better than anticipated by the DHS (2019) report. Some bridges may require repair, but bridges are likely to remain useable for emergency vehicles and post-earthquake response. The 85th percentile bent drift ratios for the bridges analyzed in the parametric study were generally less than the threshold identified for no service post-earthquake.

Limitations

These conclusions were made within the scope of the study, and there are several limitations to the study that require further investigation. The findings are limited to the bridges studied and the assumptions used in the modeling. Importantly, shear failure, shear-flexure interaction, span unseating, foundation failure, damage from soil liquefaction and lateral spreading, fatigue, and corrosion or other durability-related issues were not considered and remain important priorities for bridge seismic retrofit. Additionally, ground motions from only the CSZ source were considered, and crustal faults in the region should be considered in a complete seismic evaluation.

CHAPTER 1. INTRODUCTION

The earthquake performance of bridges is critical to the post-event mobility of nearly all transportation modes, including bicycles, automobiles, trucks, buses, and rail. Damage to bridges near critical facilities, such as airports and ports, can also limit the contributions of these facilities to the post-event mobility of people and freight. Accordingly, local, state, and federal engineers and emergency managers need reliable estimates of post-event bridge functionality in order to plan pre-event mitigation, post-event response and mobility, and long-term recovery.

Current estimates of post-earthquake bridge functionality following a Magnitude 9.0 (M9) Cascadia Subduction Zone (CSZ) earthquake were provided in a report by the Department of Homeland Security (DHS) (DHS 2019) report. This evaluation was overly simple, resulting in predictions so conservative that they are of little utility (i.e., nearly all bridges were predicted to be out of service for months and years following an M9 earthquake). Moreover, these evaluations did not account for the region's unique geologic conditions, including the presence of deep sedimentary basins that underlie most of the Puget Sound, thereby neglecting differences between bridges built in this region and elsewhere.

The goal of this project was to provide an improved prediction of post-earthquake functionality of bridges in Western Washington following a CSZ M9 earthquake. This was achieved by using several new datasets, analysis of representative bridges, and an approach formulated to assign a given bridge to a representative analysis. The results of this project could be used in a follow-up project that considered post-earthquake route demands and capacities to formally assess network mobility. The methodologies developed in this research could also be applied to other locations susceptible to strong shaking from a CSZ earthquake, such as Oregon, Northern California, Alaska, and British Columbia.

This report begins with a brief overview of background information on CSZ earthquakes and previous research conducted by the authors on the behavior of representative Western Washington bridges. A summary is then provided of the Western Washington bridge inventory. The methodology used to conduct detailed modeling of bridges in Western Washington is then described. Lastly, model analysis results are described, and scenarios of predicted bridge network functionality are presented.

CHAPTER 2. BACKGROUND

2.1. Magnitude 9.0 Cascadia Subduction Zone Fault Rupture Simulations

The Cascadia Subduction Zone (CSZ) is a 600-mile long tectonic plate boundary between the North American plate and Juan de Fuca plate, shown in Figure 2.1. Recent research has indicated that the CSZ is capable of producing a large magnitude earthquake at a return period of approximately 400 to 600 years (Pacific Northwest Seismic Network, 2021). Research on previous subduction zone earthquakes, predominately near Chile and Japan, have shown that these earthquakes can have larger spectral accelerations and durations than typical crustal earthquakes. For the CSZ, these effects may be further amplified by sedimentary basins located around Western Washington (Marafi et al, 2017). Researchers from the United States Geological Survey (USGS) and the University of Washington (UW) simulated a Magnitude 9.0 rupture of the CSZ using synthetic seismograms and 3D finite difference simulations (Frankel et al, 2018). The joint research program resulted in 30 sets of synthetic ground motions across a range of possible rupture parameters. The generated M9 motions had durations ranging from 70 to 120 seconds, with the largest spectral accelerations occurring near the Pacific coast (Frankel et al, 2018). Spectral accelerations were amplified by the presence of sedimentary basins in the Seattle area. De Zamacona Cervantes (2019) investigated the effects of the simulated, soil-adjusted M9 CSZ motions on different single degree-of-freedom models. Some models were assumed to have a strength that was 50 percent higher than the 2019 Washington State Department of Transportation (WSDOT) code-minimum value for bridges, and those models were found to suffer severe damage for short-period structures that were close to the fault. Longer-period structures were more heavily damaged if located within sedimentary basins.

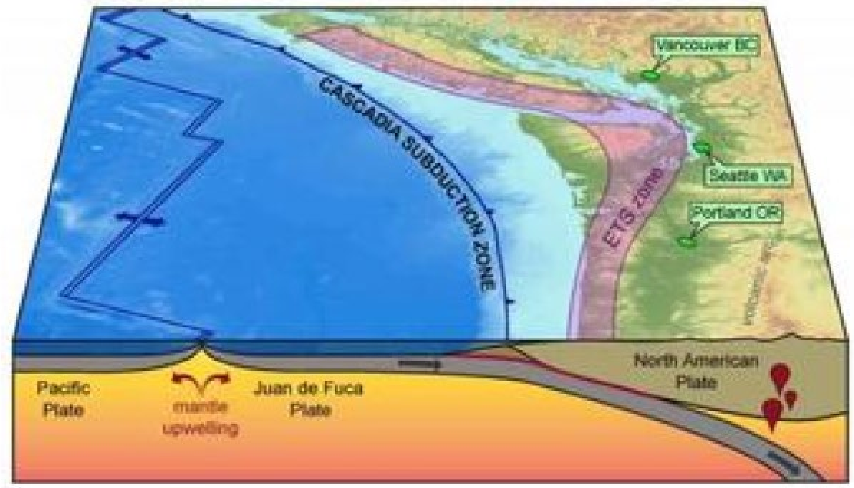

Figure 2.1 The Cascadia Subduction Zone (public domain image)

2.2. 2019 DHS RRAP Report

A DHS study (DHS, 2019) attempted to assess the functionality of approximately 2,700 bridges in Western Washington following a M9 CSZ earthquake, with results shown in Figure 2.2. That study predicted that approximately 80 percent of the bridges in Western Washington would be unavailable following an M9 CSZ earthquake, and 782 bridges would be unavailable for more than one year. This prediction has been factored into emergency planning efforts in Washington state. However, the methods used to generate those predictions were overly crude, making these estimates unreliable. The shortcomings include the following:

- reliance on metrics of ground-motion intensity that correlated poorly with bridge performance (e.g., peak ground acceleration rather than effective spectral acceleration);
- use of crude fragility relationships that were not consistent with the level of damage observed in past earthquakes (Ranf et al, 2007), fragility relationships developed by previous researchers (e.g., Gidaris et al, 2017), or damage and functionality expected by WSDOT based on the Washington Bridge Design Manual (WSDOT, 2020); and
- lack of consideration of specific bridge characteristics, such as fundamental period, when predicting performance.

A primary objective of the study summarized in this report was to rectify many of these analytical shortcomings to provide more accurate predictions of bridge functionality.

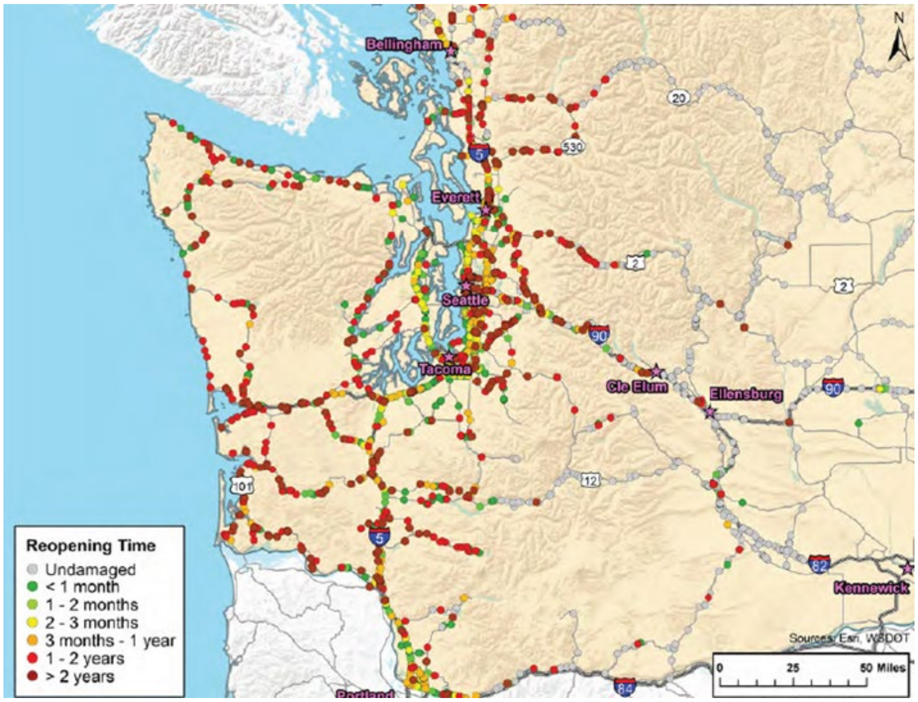

Figure 2.2 Projected bridge reopening times in Western Washington state by DHS report (DHS, 2019)

2.3. Assessment of Behavior of Washington State Bridges in a CSZ Earthquake

Significant damage to reinforced concrete bridge columns, including brittle failures, was observed following the 1971 San Fernando, California, earthquake (Fung et al, 1971). Subsequent research led to an improved understanding of the design issues, and in 1983, AASHTO issued new bridge design guidelines with changes aimed at addressing the issue of nonductile bridge columns. The seismic vulnerabilities of older bridge columns were again exposed by the 1989 Loma Prieta, California, earthquake (EERI, 1989; NIST, 1990) and 1994 Northridge, California earthquake (EERI, 1994; Buckle, 1994). Research in the 1990s (Chai et al, 1991, 1994; Priestley et al, 1994a,b) demonstrated the effectiveness of steel jackets in enhancing the ductility of older reinforced concrete bridge columns. This research was accompanied by field implementation in several states. The WSDOT implemented a seismic retrofit program in 1991, with steel jackets used as the primary means of column retrofit. In Washington state, many bridges were constructed in the 1950s and 1960s as part of the national Interstate Highway program. These include bridges for I-5, I-90, and I-405, which represent important lifelines for the city in the aftermath of a large earthquake. Roughly 50 percent of the bridges in the WSDOT seismic retrofit program have been retrofitted.

Recent studies conducted by the authors have focused on the behavior of retrofitted and unretrofitted bridges in Western Washington in CSZ earthquakes. These include an experimental study at Washington State University on six circular columns retrofitted with steel jackets (McGuiness, 2021). The columns had parameters that were intended to span the typical WSDOT inventory. The reversed-cyclic loading protocol used in the tests had more cycles than typical laboratory testing protocols to better reflect the long-duration CSZ demands. The tested columns exhibited high levels of ductility, with strength degradation occurring due to fatigue fracture of the longitudinal reinforcement. Two of the six columns were tested to a state of collapse, assessed as the inability to hold gravity load. Significant ductility was found between fist bar fracture and collapse. The reinforcement used in the test columns differed from the reinforcement used in older reinforced concrete bridge columns. Cyclic testing of individual reinforcement was conducted to assess fatigue behavior (Motter et al, 2023). The testing included reinforcement from the test columns and reinforcement obtained from 1950s-era demolished bridges. Fatigue models were fit to the test results, and the older reinforcement was found to have significantly lower fatigue life than the reinforcement used in the test columns. A column model was formulated in OpenSees, with the stress-strain history obtained from analysis and run through a fatigue model to estimate bar fracture. The model was validated with the test results and then used to conducted single-degree-of-freedom nonlinear time history analyses. For single-degree-of-freedom analyses, a single column was modeled and used to represent the behavior of the bridge. The analyses were conducted for a range of periods and a range of SaW/Fy, where Sa is the design spectral acceleration, W is the seismic weight of the bridge, and Fy is the yield strength. The results of the time history analyses were used to formulate fragility curves, which provided estimates of the probability of reinforcement fracture.

A recent study conducted by researchers at the University of Washington (UW) evaluated the predicted deformation demand of unretrofitted bridge columns for various locations around Western Washington (Kortum et al, 2021). The study used a database of bridge properties for 609 bridges located mostly along the I-5/405 lifeline that was compiled from WSDOT's bridge inventory. From the bridge property database, researchers developed nonlinear single-degree-of-freedom models that reasonably well represented the spread of bridge period, stiffness, and strength. The nonlinear single-degree-of-freedom model was formulated in OpenSees (Mazzone et al, 2006) using the Modified Ibarra-Medina-Krawinkler (IMK) deterioration model with peakoriented hysteretic response material (Lignos and Krawinkler, 2012; Kortum et al, 2021). The IMK model used input parameters to control the backbone of the force-displacement behavior, and these parameters were calibrated by Kortum et al (2021) to match the measured force-displacement response of three reinforced concrete column tests in the UW-PEER structural performance database. The three tests comprised a lightly reinforced column, a moderately reinforced column, and a heavily reinforced column. In general, the IMK models accurately predicted the cyclic behavior and deterioration of the column tests and were deemed sufficiently accurate. Nonlinear time history analyses were then conducted using the models in combination with ground motions for ten locations across Western Washington for 30 M9 CSZ scenarios for four different site classes. The analyses determined that, on soft soils, bridges with periods of above 0.4 to 0.7 seconds had the largest spectral accelerations, deformation demand, and expected damage. For stiffer soils, bridges with shorter periods tended to have the highest demands. Bridges with one standard deviation below median strength had deformation demands approximately 50 percent larger than that of the median strength bridges. The acceleration response spectra for the coast were very high, with values near 2.0g. This was due to proximity to the fault, as coastal locations lack sedimentary basins. For bridges with periods of between 0.2 and 2.0 seconds, the likelihood of concrete spalling was from 35 to 50 percent for site class C soil. For bridges located away from the CSZ and outside of sedimentary basins, the spectral acceleration was low, ranging from 0.5g to 1.0g, and the likelihood of concrete damage was low for all conditions. For bridges within the sedimentary basins, performance was strongly linked to the fundamental period. For bridges with periods of between 0.5 and 3 seconds, the likelihood of concrete spalling was between 50 and 75 percent.

Both of these previous studies used single-degree-of-freedom analyses for representative bridges. In this study, a multi-degree of freedom bridge model was formulated and used for analysis of representative bridges, and the performance of actual bridges in the Western Washington state inventory was assessed.

CHAPTER 3. DATA AND METHODS

3.1. Expansion of the WSDOT Bridge Database

The Washington State DOT compiled a database of bridge properties along the primary lifeline routes of I-5, I-405, and I-90 in the Seattle area. The database included information for 609 highway bridges, located as shown in Figure 3.1. For each bridge in the WSDOT database, the parameters collected were year of construction, superstructure type, column dimension, transverse and longitudinal reinforcement ratio, span lengths, and number of piers. Column properties were included for the tallest and shortest columns on the bridge.

Figure 3.1 Locations of bridges along I-5, I-405, and I-90 (Kortum et al, 2021)

During this project, the existing WSDOT bridge database was expanded to include 58 additional bridges, as well as additional parameters for abutments, shear keys, and site class. The additional bridges were multi-span, reinforced concrete column bridges on secondary routes, including State Route (SR) 101, 12, 16, and 3, mostly to the west of I-5. Information on shear keys was added for each of these bridges. The additional parameters on abutments were added for 114 bridges. The abutment parameters included information on abutment type and foundation type. Site class was determined for all bridges in the database, based on latitude and longitude coordinates and the Vs30 soil model developed by Geyin and Maurer (2023). The expansion of the WSDOT bridge database excluded single-span bridges, pier wall bridges, steel truss bridges, and special project bridges, such as suspension bridges. Single-span bridges were excluded on the basis that these bridges are likely to survive any earthquake if unseating and abutment failure are prevented.

Most of the bridges along major highways in the Puget Sound region were built before the incorporation of ductile detailing. Of the 582 bridges documented in the original WSDOT database, 435 (74.7 percent) were built before 1976. The year 1976 is important in seismic engineering, as it is the year in which seismic detailing of reinforced concrete columns was significantly improved in response to the 1971 San Fernando earthquake. Therefore, bridges designed after 1976 are likely to be more capable of resisting larger deformations than pre-1976 bridges. A total of 74 bridges had a single span, whose failure mode tends to be span unseating, which early WSDOT retrofit efforts have targeted. Out of 508 bridges with multiple spans, 416 (71.6 percent) of the intermediate supports contained at least one reinforced concrete column, which is a common location of bridge damage and failure. As expected, the transverse reinforcement ratio for older reinforced concrete columns (pre-1976) tended to be much smaller than for newer columns, but the longitudinal reinforcement ratio did not vary greatly based on the era of construction.

The additional 58 bridges added to the database ranged in year of construction from 1948 to 2018, with 48 percent being built before 1976. Of the multi-span bridges on the secondary routes examined, five of the 58 were supported by single-column bents, while the rest were supported by multi-column bents. The majority of the secondary route bridges were similar to the lifeline route bridges, with average column heights of between 6 and 30 feet, and three with column heights of greater than 40 feet. The secondary route bridges had common column diameters of between 11 and 20 inches, which was smaller in diameter than the lifeline route bridges, which were more commonly between 31 and 40 inches. Only one secondary route bridge added to the database had been seismically retrofitted with steel jackets. The most common bridge configuration was three spans. Longitudinal and transverse reinforcement ratios were generally consistent with data for the original WSDOT database. The secondary route bridges were generally similar to the lifeline route bridges, with the exception of smaller column diameters and a prevalence of multi-column bents over single-column bents.

3.2. Multi-Degree-of-Freedom Bridge Model

A multi-degree-of-freedom bridge model was formulated and used to conduct analyses for representative bridges in Western Washington. The numerical modeling strategies used for the multi-degree-of-freedom bridge model were extended from and built upon the work of Ranf et al (2007), Ramanathan (2012), and Mangalathu et al (2019). A schematic of a typical highway reinforced concrete bridge is provided in Figure 3.2. The superstructure of the bridge comprises the deck slab, traffic barriers, and girders. The substructure comprises intermediate bent supports, abutments, shear keys, and bearings, depending on the type of the bridge abutment. The intermediate bent supports typically consist of cross-beams, columns, and foundation. The numerical models used for these key components and assembly of these components into a complete bridge model and described in this section. The three-dimensional numerical bridge model was formulated in OpenSeesPy (Zhu et al, 2018), a Python-compiled version of OpenSees (Mazzoni et al, 2006).

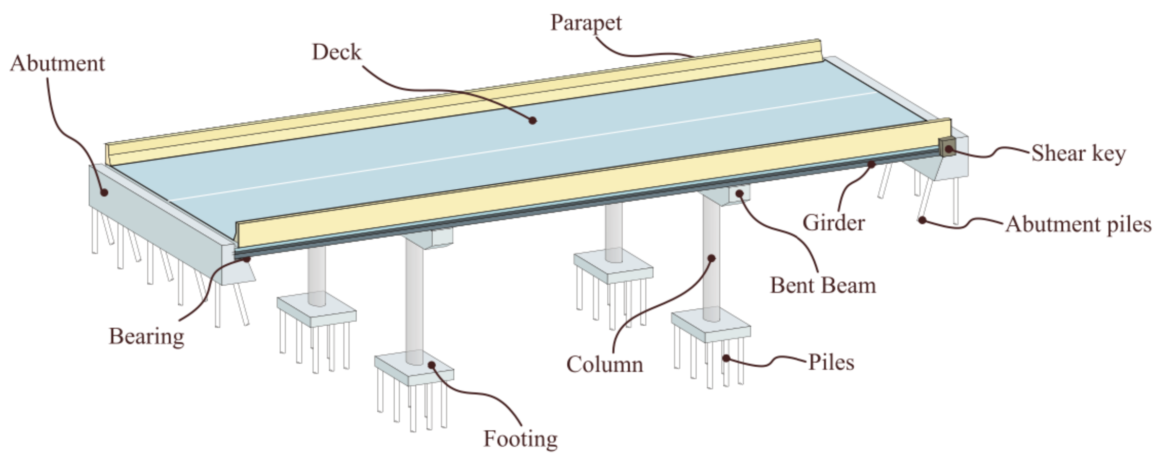

Figure 3.2 Typical highway concrete bridge components (Mangalathu, 2017)

A schematic of the overall bridge model is provided in Figure 3.3. The superstructure was modeled as a spine of elastic beam-column elements, as the bridge deck was expected to remain elastic during earthquake response. The mass of the superstructure was uniformly assigned to the longitudinal deck nodes according to the tributary area of the deck and the length of the traffic barrier. Rigid offsets were used from the centerline spine to the intermediate bents and abutments. The rigid offsets were modeled as stiff and massless elastic beam-column elements that extended perpendicularly from the spine to the full deck width. Rigid links were similarly used to connect the extension of the deck to the top of columns. Intermediate bents included cross-beams, columns, and foundations, as shown in Figure 3.4, and were modeled with a combination of nonlinear beam-column elements and rigid links. The model for the circular columns is shown in Figure 3.5. Inelastic flexural response was modeled by using distributed plasticity forced-based beam column elements (nonlinearBeamColumn), which required cross-sections to be defined at each of the integration points. Concrete04 and Steel02 material models in OpenSeesPy were used for concrete and reinforcement in the fiber-sections. Elastic shear and torsional were aggregated to the cross-sections by using the Section Aggregator command in OpenSeesPy. Zero-length fiber sections were used at the top and bottom of the columns to simulate rotational flexibility resulting from bond slip of the longitudinal column reinforcement. Rotational and translational springs were used at the base of the columns to model foundation behavior. The rotational spring stiffness and translational spring stiffness were 7*106 kip-in/rad and 1300 kip/in, respectively, based on Ramanathan (2012).

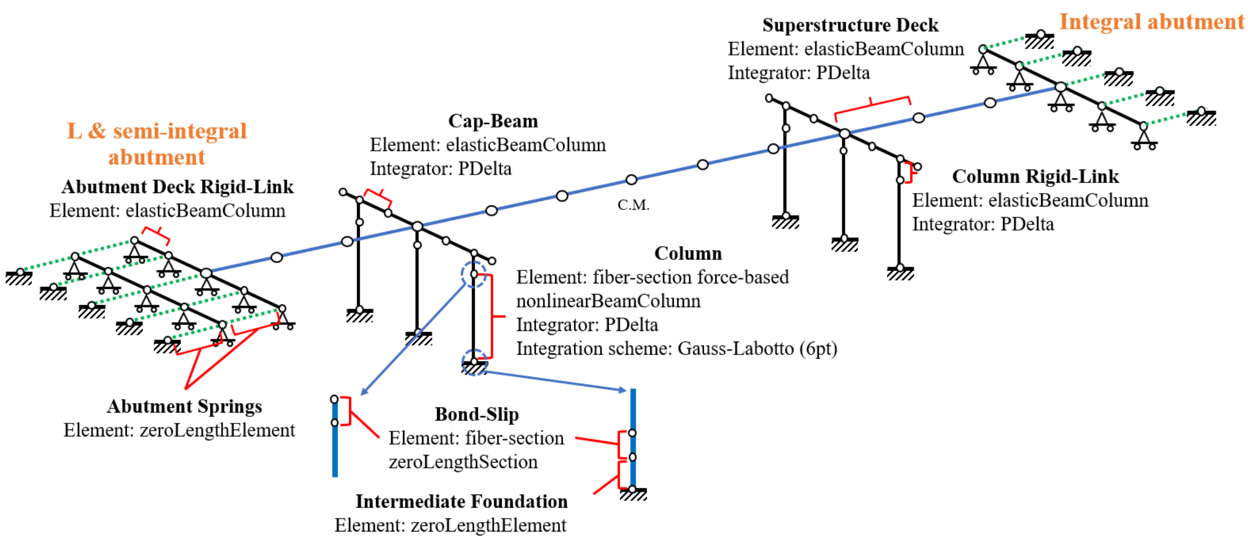

Figure 3.3 Multi-degree-of-freedom bridge model

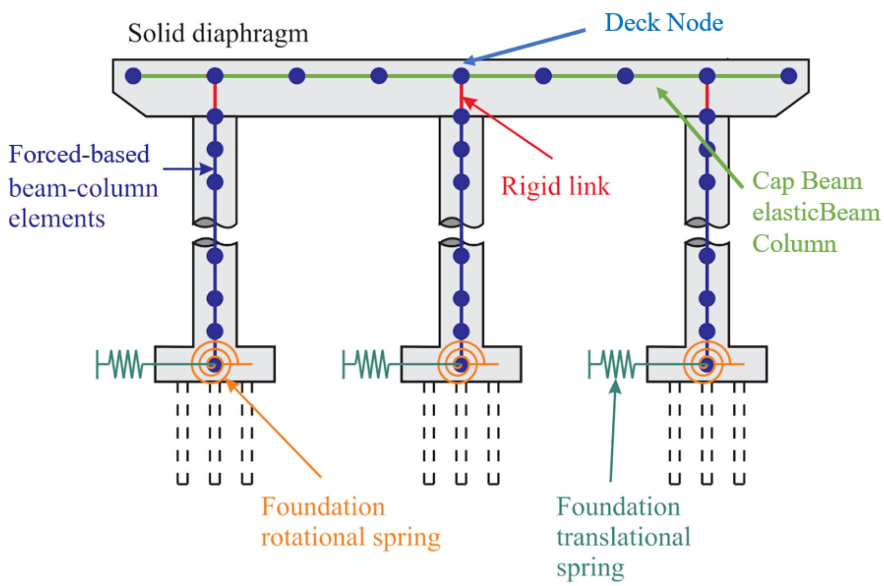

Figure 3.4 Finite element discretization of the bents (Ramanathan, 2012)

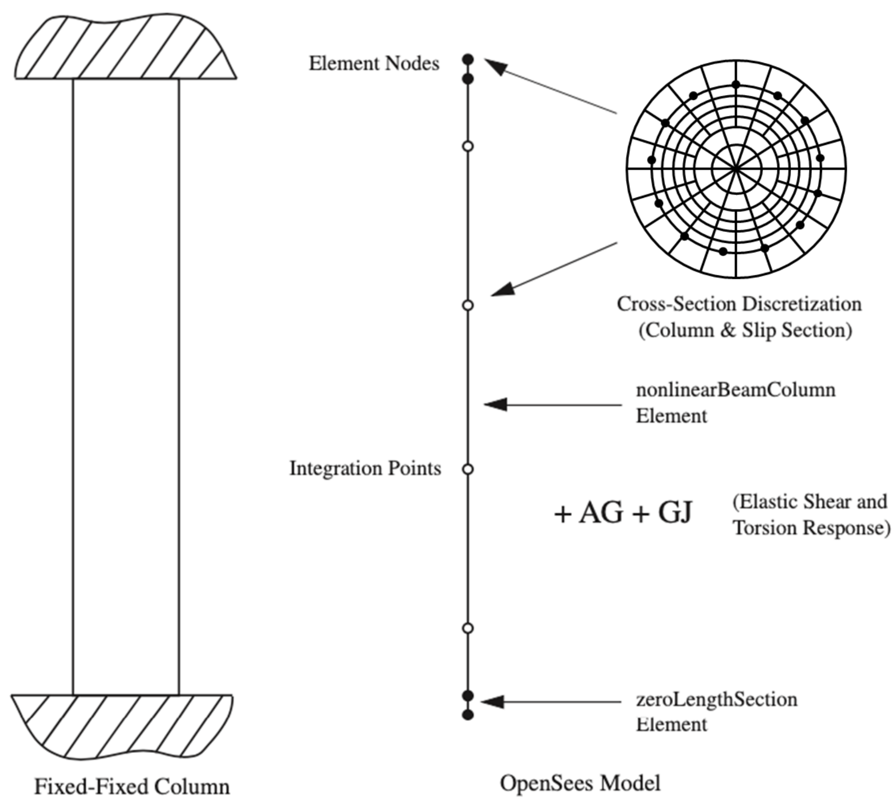

Figure 3.5 Components of the numerical column model (Ranf, 2006)

Three different types of abutments—namely integral, semi-integral, and L (seat) abutments—were used in this study. Integral abutments are cast monolithically with the superstructure and restrict deck movement in both the transverse and longitudinal directions. Integral abutments have high stiffness, limited only by the backfill soil and the abutment foundations. Semi-integral abutments are not cast monolithically with the superstructure but have the same behavior in the longitudinal direction, as the deck goes beyond the abutment backwall and engages directly with the backfill soil. In the transverse direction, semi-integral and L abutments provide bearing support to the superstructure, with movement restrained by shear keys at both ends of the bridge. For L abutments, the longitudinal motion of the superstructure is restrained by bearing pads, the abutment backwall, and the backfill soil. In the model, two different spring systems consisting of zero-length elements were used, as shown in Figure 3.6. Although semi-integral and L abutments use the same type of spring systems, the stiffness of the bearing springs differ in the longitudinal direction, with the former modeled as rigid and the latter as flexible. For semi-integral and L (seat) abutments, a zero-length element was connected in series with the backfill element to model pounding between the backfill soil and deck. Zero-length elements for the shear keys and bearing pads were used in parallel with the pounding elements. For integral abutments, zero-length elements were used for backfill soil, and bi-directional forces (abutment piles/spread footings and friction surface) were connected in parallel and linked to the ends of the deck elements. The passive response of the abutment backwall was captured by a hyperbolic soil model established by Shamsabadi and Yan (2008).

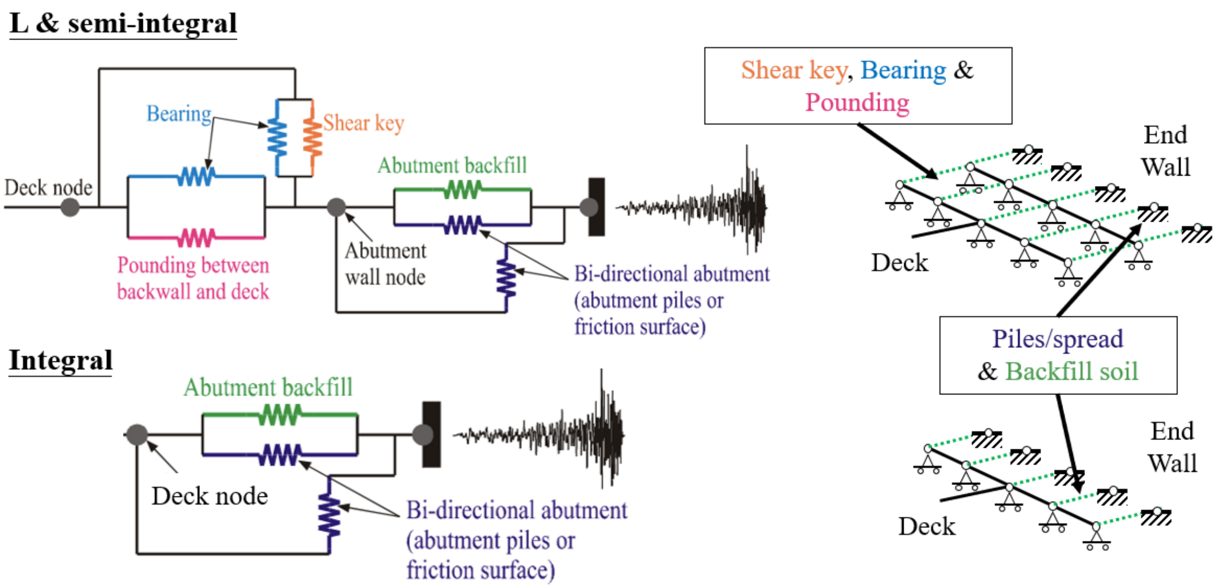

Figure 3.6 Zero-length spring system for L, semi-integral, and integral abutments

3.3. CSZ Ground Motions Used for Analysis

The suite of bridge models was analyzed for the set of 30 simulated CSZ ground motions at ten locations across Western Washington, with each motion at each location containing two orthogonal components (Frankel et al, 2018; De Zamacona Cervantes, 2019). The locations of the ten sites are shown in Figure 3.7 and described in Table 2.1. The median response spectra for each of the ten sites is provided in Figure 3.8. The coastal cities of Forks and Ocean Shores, where many of the secondary routes analyzed in this study were located, had high spectral accelerations at periods of 0 to 1.0 second. Additionally, the effect of the sedimentary basins was evident between periods of 1.0 to 3.0 seconds, where the spectral acceleration maintained a relatively high value before decreasing. The baseline (Frankel et al, 2018) and soil-adjusted M9 ground motions (De Zamacona Cervantes, 2019) were used to conduct parametric studies to investigate the performance of bridges in Washington state. Six representative cities were selected to consider four geological conditions in Western Washington state: coastal outside of basin (Forks and Ocean Shores), inland shallow basin (Port Angeles), inland outside of basin (Olympia), and inland deep basin (Seattle and Everett).

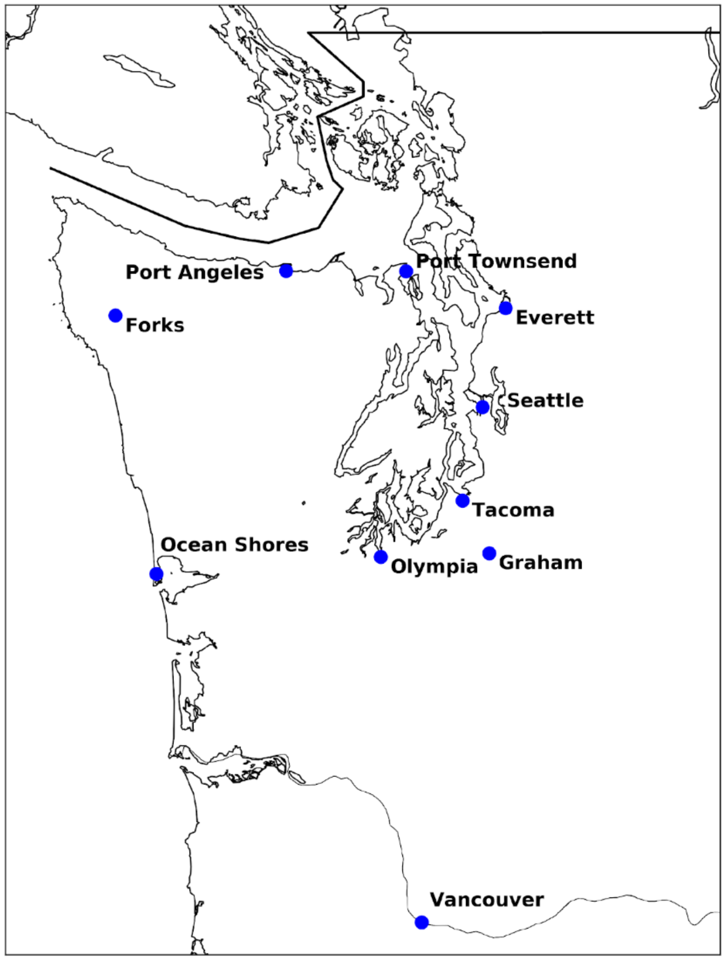

Figure 3.7 Locations of ten sites for analysis (De Zamacona Cervantes, 2019)

Table 2.1 Selected sites and nearest station (from Frankel et al. 2018)

City Name	Station ID	Latitude	Longitude
Forks	Z0FORK	47.9456	-124.566
Ocean Shores	Z0XOCS	46.9778	-124.154
Port Angeles	Z0XANG	48.1191	-123.431
Olympia	Z00CPW	46.9717	-123.138
Port Townsend	Z0XTWN	48.1146	-122.756
Vancouver	Z0HUBA	45.6287	-122.653
Tacoma	Z0TBPA	47.2559	-122.368
Seattle	Z0XWLK	47.6120	-122.338
Graham	Z00GHW	47.0395	-122.274
Everett	Z0EVCC	48.0056	-122.204

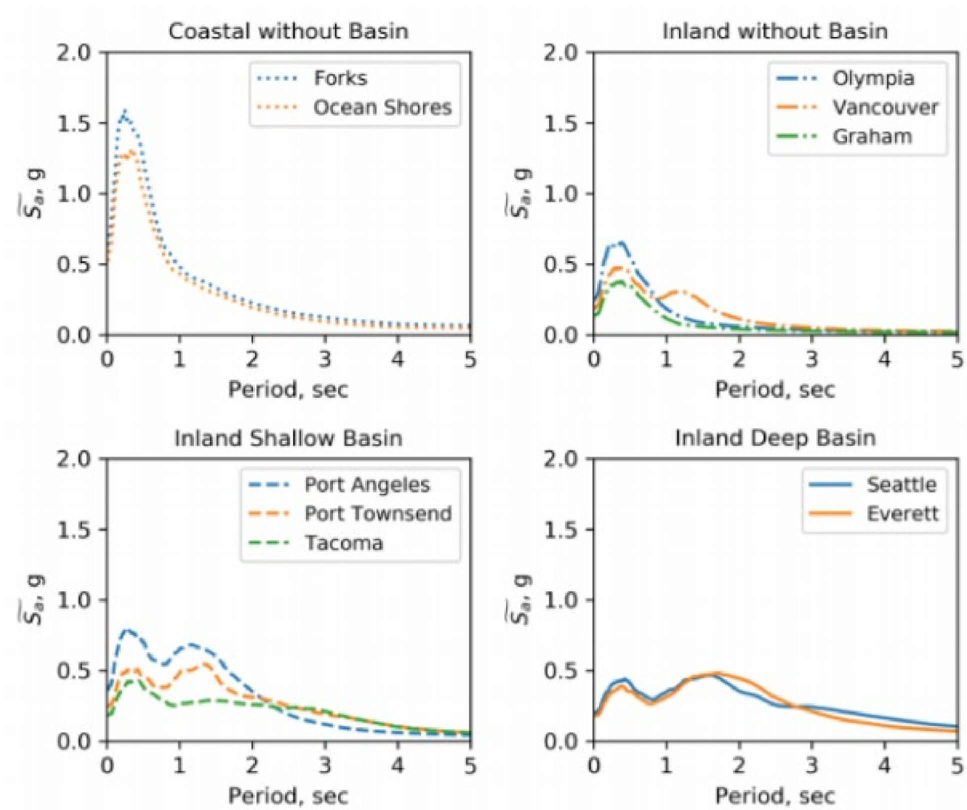

Figure 3.8 Response spectra of 10 sites for analysis (De Zamacona Cervantes, 2019)

3.4. Parametric Studies

Nonlinear time history analyses were conducted for several representative bridges. A reference bridge was used as a starting point, and parameters were varied to create other representative bridges. This parametric study included variation in geographic location (Forks, Ocean Shores, Port Angeles, Olympia, Seattle, and Everett), site class (C2, C4, D1, D3), column height and transverse reinforcement, and abutment properties such as abutment configurations (L, semi-integral, and integral abutment), abutment foundation types (spread footings, piles), shear keys (present or absent), bearings (present or absent), and soil types (medium sand and medium clay). Bridges without shear keys but with bearing pads represented bridges without shear keys, while bridges without shear keys and without bearing pads represented bridges that were not continuous.

3.5. Predicting Bridge Functionality

The analyses described in the previous section were conducted for representative bridges. A procedure was needed to assign bridges to representative analyses or to otherwise characterize the performance of actual bridges in a CSZ earthquake. Similar to the procedure used in the DHS (2019) report, three expected post-earthquake service levels were defined. These included

1) Full service – full access to ordinary traffic is available almost immediately after the earthquake,
2) Limited service – bridge is open for emergency vehicle traffic, and a reduced number of lanes for ordinary traffic is available within three months of the earthquake, and
3) No service – bridge is closed for repairs and replacement.

Because expected post-earthquake bridge service is the more critical finding for emergency planning, it was used as the primary reporting measure for this study. Full service bridges would be open for emergency vehicles, evacuations, and movement of supplies directly after the earthquake. Limited service bridges would likely be open for emergency vehicles and movement of supplies for emergency response but would not be open for traditional traffic until approximately three months after the earthquake. No service bridges were assumed to be non-functional and, therefore, would prevent passage of any vehicle.

For bridges with unretrofitted columns, assessment of functionality was based on the results of bridge analyses from the previous section. Bridges with retrofitted columns were characterized as full service. A previous study (Motter et al, 2023) included fragility curves for the lateral failure of retrofitted columns, with lateral failure defined as a 20 percent loss of lateral load resistance. This previous study found that lateral column failure was more likely for shorter period bridges near the coast and longer period bridges in sedimentary basins, such as that underlying much of the Seattle region. This previous study did not include analytical assessment of collapse probability, as the likelihood of collapse was assessed to be low based on test results, with the tested columns exhibiting significant deformation capacity after lateral failure to reach axial failure (i.e., collapse). Fatigue fracture of longitudinal reinforcement was the primary means of strength degradation observed in the tests; that is, the circular layout of the longitudinal reinforcement likely promoted ductility in the test columns after lateral failure, which was associated with fracture of the first longitudinal bar.

CHAPTER 4. FINDINGS

A key question addressed in this study was the effectiveness of the abutments in restraining the expected deformations of the bridge. This restraint depends greatly on the continuity of the superstructure and on the presence of transverse shear keys at the abutments. The database study found that 76 percent of pre-1976 bridges had continuous superstructures, and this percentage increased to 97 percent for modern bridges (1976-present). A study of a subset of 94 bridges found that 90.3 percent (65 of 72 bridges) of the older bridges and 100 percent (19 bridges) of the newer bridges had an internal or external shear key.

The simulated deformation responses of the reference bridge, provided in Figure 4.1, in the longitudinal direction were consistently smaller than those in the transverse direction because of the high resistance provided by the abutment and backfill soil. For all six locations and four site classes, the 85th percentile bent drift ratio was below 1.0 percent. In the transverse direction, the coastal locations (Forks and Ocean Shores) had the largest displacement responses. The highest responses in coastal cities were for site class D1, with the 85th percentile responses reaching values of almost 2.5 percent for the maximum bent drift ratio. The responses tended to decrease as the distance from the coast increased. The median bent drifts were less than 0.8 percent for the two cities located far from the coast and on deep basins (Seattle and Everett). For these two locations, the responses consistently increased as the site became softer, reaching a maximum value for site class D3, but the 85th percentile values never exceeded a 1.0 percent drift ratio at the bents. Bridges with less flexibility were observed to have the largest deformation response in cities closer to the coast (Ocean Shores), whereas those with higher flexibility had the largest response in the inland city on the sedimentary basin (Port Angeles), especially for ground motions generated with the softest soil site class (D3). This observation was consistent with expected effects of basin amplification. In cities away from the coast, the motions were not found to be strong enough to cause yielding and softening of the bridge; thus their response was smaller than that for cities closer to the coast.

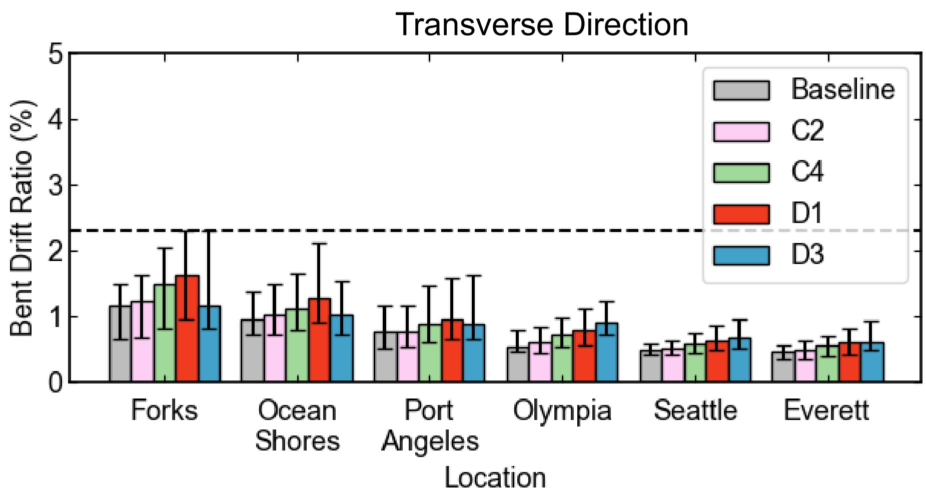

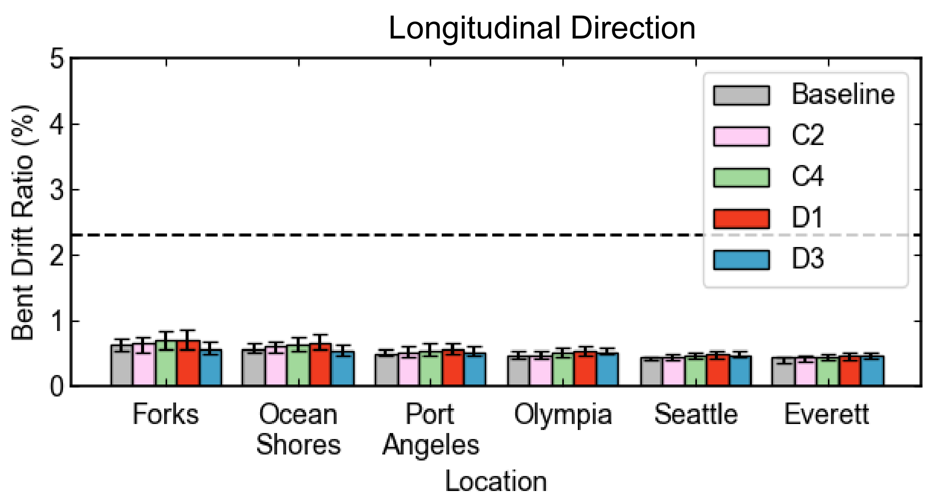

Figure 4.1 Maximum bent drift ratio for median, 15th, and 85th percentiles

The displacement demands in Figure 4.1 were compared with estimates of the deformations at the onset of column spalling and bar buckling. These two damage states are important because spalling generally represents the first visible damage to a column that may require repairs, whereas bar buckling represents a more severe form of damage that may require long-term bridge closure and expensive repairs. The median drift ratios for both damage levels were computed following the recommendations of Berry and Eberhard (2007) as:

$$\frac{\Delta_{sp,calc}}{H_{col}}(\%) = 1.6\left(1 - \frac{P}{A_g f_c'}\right)\left(1 + \frac{L}{10D}\right) \qquad (6\text{-}1)$$

where the axial-load ratio, P/(Agf'c), was taken as 0.05, and the ratio of the distance to inflection point, normalized by the column depth, was taken as 21.3 ft / 4 ft = 5.3. The resulting calculated mean drift ratio at spalling was 2.3 percent, which is shown as a horizontal, dashed line in Figure 4.1. In the longitudinal direction, the 85th percentile bent drift ratios were below the mean spalling value for all cities and soil classes. In the transverse direction, the median values never exceeded 2.3 percent, but the 85 percent values did reach this value for the two coastal cities (Forks, Ocean Shores) for site classes D1 and D3. Similarly, the mean drift ratio at the onset of bar buckling was calculated following the recommendations of Berry and Eberhard (2005), where the median drift ratio causing bar buckling is given by:

$$\frac{\Delta_{bb,calc}}{H_{col}}(\%) = 3.25(1 + k_{e,bb}\rho_{eff}\frac{d_b}{D})(1 - \frac{P}{A_g f_c'})(1 + \frac{L}{10D}) \qquad (6\text{-}2)$$

where ke,bb was taken as 150, ρeff was taken as 0.005 for an old bridge, and the ratio of the longitudinal bar diameter to the column depth, db/D, was taken as 0.0376. Based on Equation (6.2), the mean drift ratio at the onset of bar buckling was 4.9 percent. This drift ratio exceeded the 85th percentile values of the bent deformation demands for all combinations of locations and site classes.

As shown in Figure 4.2, the type of abutment did not significantly affect the transverse response of the bridge, with the median bent drift consistently between 0.5 percent and 1.5 percent. The L-type abutment and the semi-integral abutment produced similar displacement responses. On the other hand, the integral abutments tended to produce smaller responses, as integral abutments restrain transverse displacement because of the lack of a gap between the bridge deck and the shear keys. The abutment foundation type and the associated soil type had small impact on the bridge response. The spread footings allowed more transverse displacement relative to the pile, but the magnitude of the increase was dependent on ground motion realization. There was a slight increase in the median bent drift ratio, but it still never exceeded 1.5 percent. However, the variability in the response increased significantly, as the 85th percentile value for bent drift ratio was greater than 5 percent for the bridge with spread footings on medium clay. The force demands on the internal transverse shear keys tended to be far below their nominal capacity. For most scenarios that were considered in this research where shear keys were present, the 85th percentile values for the sum of the column forces were close to or just reaching the effective yield of the columns.

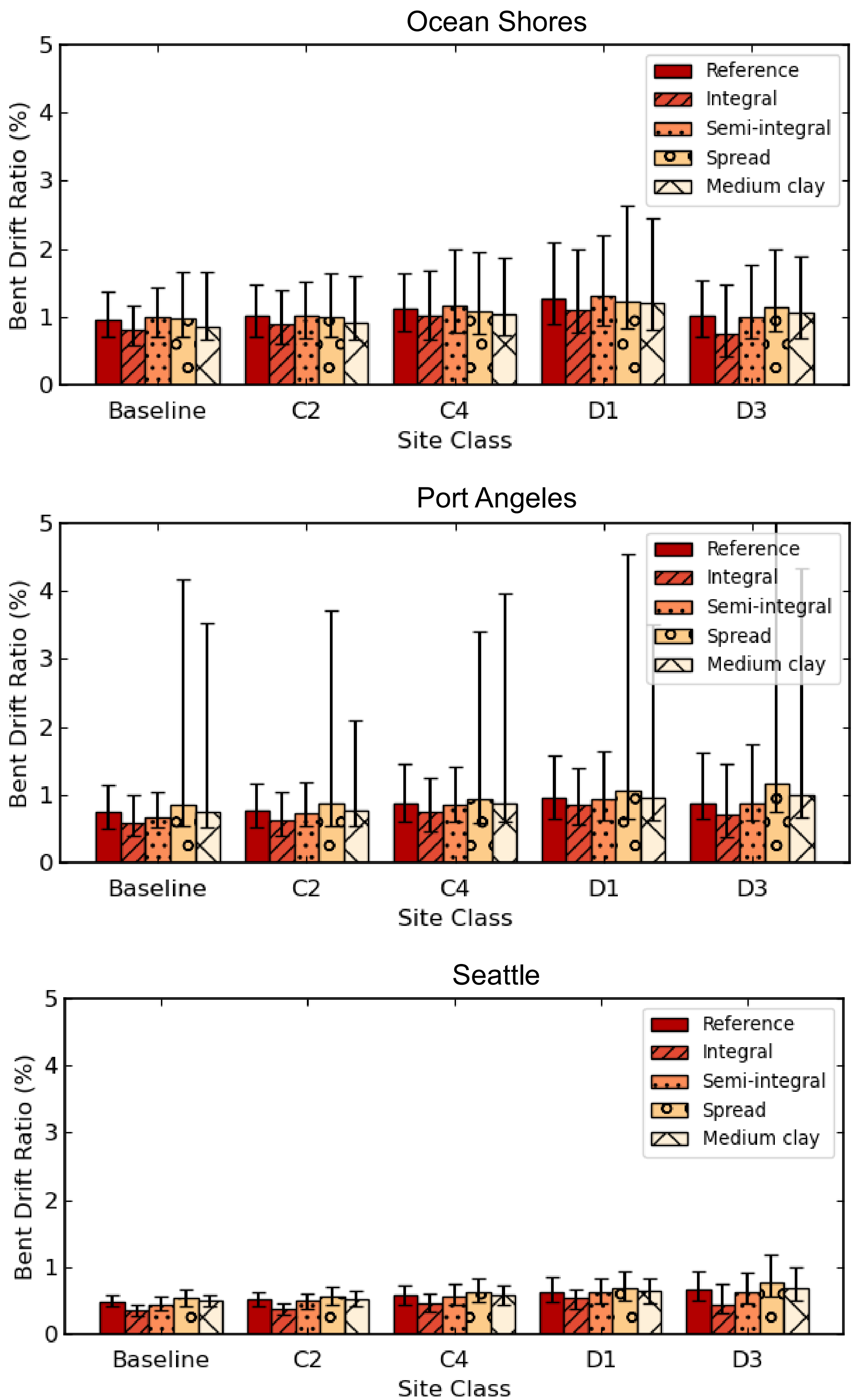

Figure 4.2 Maximum bent drift ratios for median, 15th, and 85th percentiles, with variations in abutment type and site class

A significant increase in transverse displacement response was found with removal of the shear keys and bearing pads, as shown in Figure 4.3. When both the shear keys and bearing pads were removed, the median bent drift ratio was more than three times higher than the original value for the reference bridge. This condition, with the shear keys and bearings removed, indirectly approximated the response of bridges with discontinuous superstructures, and the results indicated that such bridges are likely to have severe damage. When the shear keys were removed and the column height was doubled, the median bent drift ratio further increased, as shown in Figure 4.4, to nearly five times that obtained for the reference bridge. The increase was largest for cities on top of sedimentary basins, with the highest median drift ratio over 2 percent and the 85th percentile close to 5 percent. This indicates that discontinuous bridges with tall columns should be prioritized for seismic evaluation and retrofit. Decreasing the column height also influenced the response significantly when the shear keys and bearings were not present. When the column height was reduced to half the column height of the reference bridge, the median sum of column forces was observed to increase to twice the value of the reference bridge. This indicates that shorter columns could have shear failure problems and should be prioritized for seismic evaluation and retrofit.

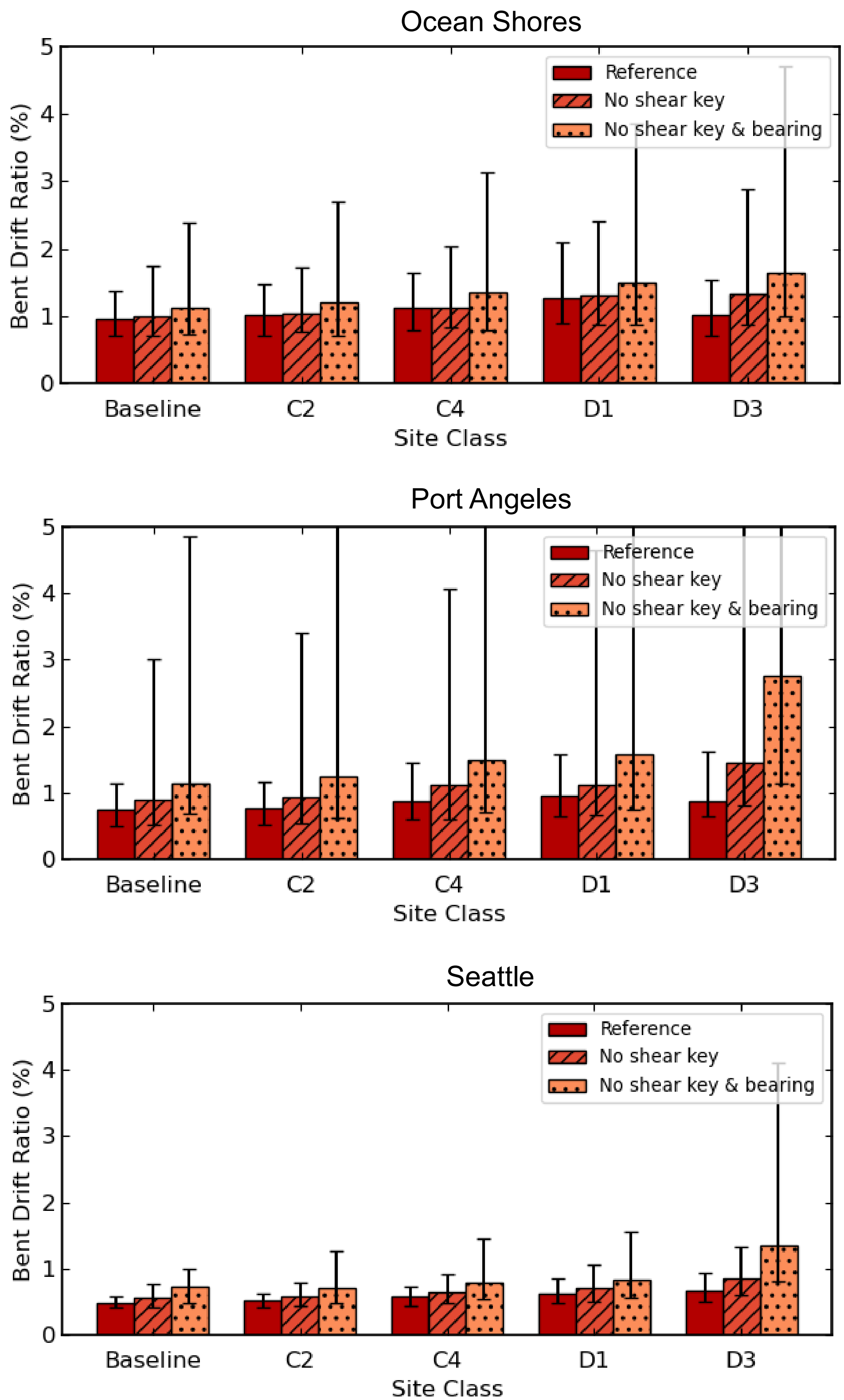

Figure 4.3 Maximum bent drift ratios for median, 15th, and 85th percentiles, with variations in inclusion or exclusion of shear keys and bearing pads

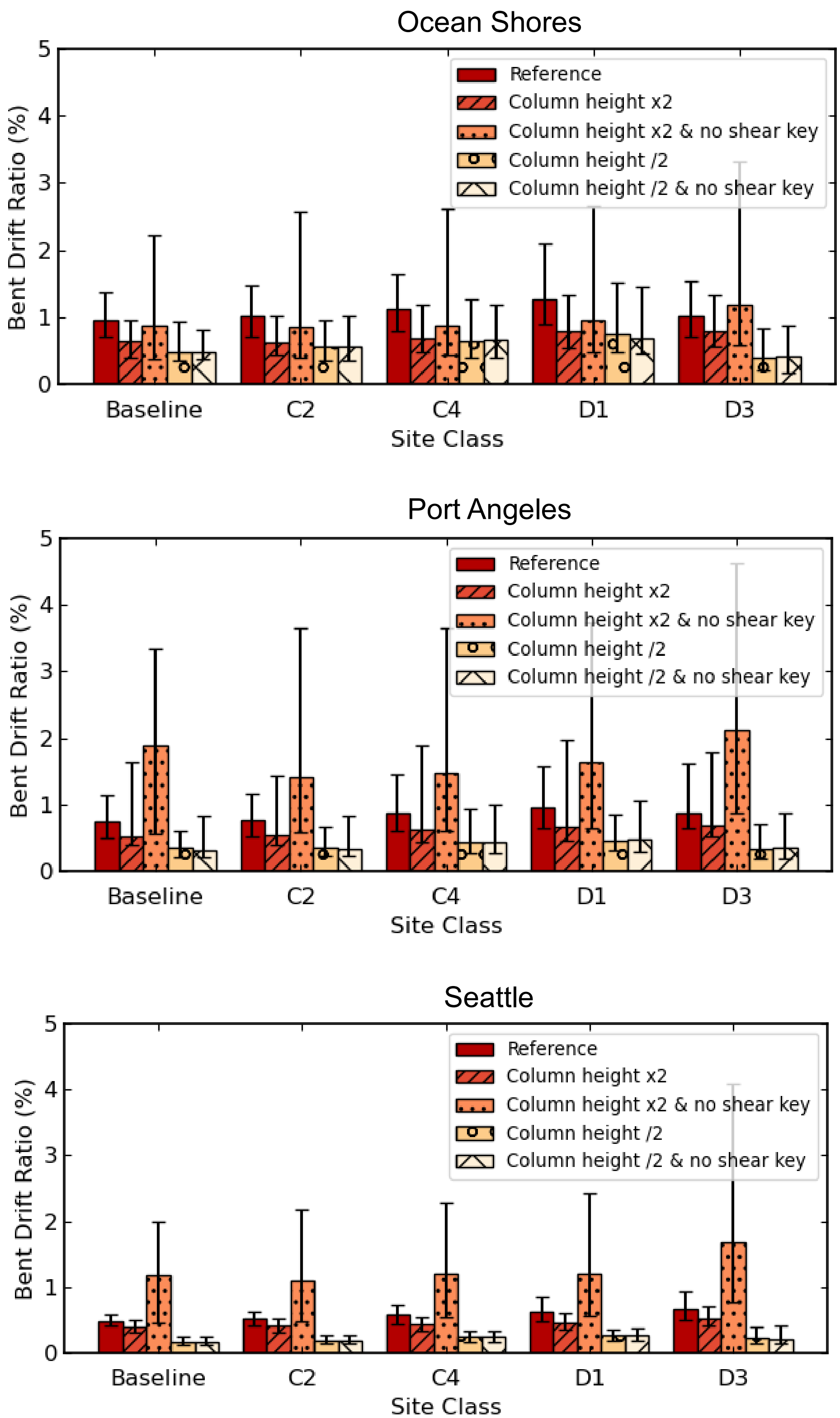

Figure 4.4 Maximum bent drift ratios for median, 15th, and 85th percentiles, with variations in column height and inclusion or exclusion of shear keys

For the case of shear keys and bearing, the median and 85th percentile bent drift ratios were less than 2.3 percent for all bridges considered in the parametric study, with 2.3 percent being the previously mentioned threshold for concrete spalling. Therefore, bridges in the WSDOT inventory with shear keys and bearing were characterized as full service. For bridges with shear keys and bearing, median bent drift ratios were less than 2.3 percent for all bridges considered in the parametric study, and the 84th percentile values were generally less than 4.9 percent, which was the previously mentioned threshold for bar buckling. Therefore, given median values, bridges without shear keys and continuity were characterized as full service based on median values and classified as limited service based on 85th percentile values.

These results suggest a significantly different post-earthquake serviceability for the Washington bridge network than that reported by the DHS (2019). The likelihood of widespread significant bridge damage is relatively low. Within the limitations of the study, the results suggest that the emergency management plan of Western Washington can likely rely on ground transportation modes to transport resources and people across the state or to the I-5/405/90 lifeline.

CHAPTER 5. SUMMARY AND CONCLUSIONS

The behavior of bridges in Western Washington in a Magnitude 9.0 Cascadia Subduction Zone earthquake was assessed in this study. Research on previous subduction zone earthquakes, predominately near Chile and Japan, have shown that these earthquakes can have larger spectral accelerations and duration than typical crustal earthquakes. For the Cascadia Subduction Zone, further amplification of ground motions may occur because of sedimentary basins in Western Washington. A DHS study (DHS, 2019) attempted to assess the functionality of bridges in Western WA following a Magnitude 9.0 CSZ earthquake, predicting that approximately 80 percent of the bridges in Western Washington would be unavailable. However, the methods used to generate these predictions were overly crude, making these estimates unreliable. A primary objective of the study summarized in this report was to conduct more refined analyses that could be used to provide more accurate predictions of bridge functionality.

In this project, the WSDOT bridge database was expanded to add the properties of 58 additional bridges located on secondary routes that feed into the I-5/405/90 lifeline. Those bridges were primarily located west of I-5, with the majority on the Olympic Peninsula. In addition to the added bridges, the WSDOT bridge database was expanded to include properties of abutments and foundations, and the site class for each bridge was identified. The properties of the bridges in the database were used to define the parameters for a parametric study on Western Washington bridges subjected to Magnitude 9.0 CSZ ground motions. Detailed multi-degree-of-freedom bridge models were developed using OpenSees. The models included abutments, foundations, soil stiffness, and the influence of shear keys between girders, when present. A model was formulated for a representative bridge with parameters varied to model a suite of representative bridges. The models were analyzed for 30 scenarios of CSZ earthquakes at ten locations across Western Washington. Results from the model analyses were used to provide a more detailed understanding of the likelihood of bridge damage and the likely service levels post-earthquake.

Within the scope of the study, the following conclusions were made, which WSDOT and Washington State emergency planning officials can use to better prepare for a possible Magnitude 9.0 CSZ earthquake:

- The response of the bridges was considerably different in the longitudinal and transverse directions. In the longitudinal direction, the response was limited because of the presence of the abutment and backfill soil, which provided sufficient stiffness to limit the motions. Single-degree-of-freedom models that neglect the effects of the stiffness provided by the abutments and backfill (e.g., models that include only the column stiffness) are likely to result in significant over-prediction of bridge deflections in the longitudinal direction. Upon observing the influence of the abutments and backfill on limiting the bridge motion in the longitudinal direction, analyses focuses more on the response in the transverse direction.

- In the transverse direction, the influence of shear keys and bearings on bridge response was significant. Bearings reflect a continuous bridge deck, and shear keys allow the columns to engage with the bridge deck so that the bridge deck provides stiffness in the transverse direction by going into bending. The stiffness provided by the bridge deck was found to significantly limit lateral deformation in the columns.
- For bridges with shear keys and bearings, the median and 85th percentile bent drift ratios were less than the threshold identified for concrete spalling for all bridges considered in the parametric study. Bridges in the WSDOT inventory with shear keys and bearings were predicted to be in full service following a CSZ earthquake. The majority of the bridges in the WSDOT inventory have shear keys and bearings.
- WSDOT has been retrofitting older reinforced concrete bridge columns since 1991. Bridges with retrofitted columns were predicted to be in full service following a CSZ earthquake. This conclusion was based on previous research that showed a low likelihood of failure for these columns.
- Bridges without shear keys and bearings should be prioritized for retrofit. Shorter period bridges near the coast and longer period bridges in locations with sedimentary basins, such as Seattle and Port Angeles, were identified as being more prone to damage.
- Bridge functionality after a CSZ earthquake is likely to be considerably better than anticipated by the DHS report (2019). Some bridges may require repair, but bridges are likely to remain useable for emergency vehicles and post-earthquake response. The 85th percentile bent drift ratios for the bridges analyzed in the parametric study were generally less than the threshold identified for no service post-earthquake.

These conclusions were made within the scope of the study, and there are several limitations to the study that require further investigation. The findings are limited to the bridges studied and the assumptions used in the modeling. Importantly, shear failure, shear-flexure interaction, span unseating, foundation failure, damage from soil liquefaction and lateral spreading, fatigue, and corrosion or other durability-related issues were not considered and remain important priorities for bridge seismic retrofit. Additionally, ground motions from only the CSZ source were considered, and crustal faults in the region should be considered in a complete seismic evaluation.

REFERENCES

Berry, M.P., and Eberhard, M.O. (2005). Practical Performance Model for Bar Buckling. Journal of Structural Engineering, 131(7): 1060-1070.

Berry, M.P., and Eberhard, M.O. (2007). Performance Modeling Strategies for Modern Reinforced Concrete Bridge Columns. PEER-2007/07, Pacific Earthquake Engineering Research Center, University of California, Berkeley, CA.

Buckle, I. G. (1994). The Northridge, California Earthquake of January 17, 1994 Performance of Highway Bridges. Technical Report NCEER-94-0008, National Center for Earthquake Engineering Research.

Chai, Y. H., Priestley, M. J. N., and Seible, F. (1991). Seismic Retrofit of Circular Bridge Columns for Enhanced Flexural Performance. ACI Structural Journal, 88(5): 572–584.

Chai, Y. H., Priestley, M. J. N., and Seible, F. (1994). Analytical Model for Steel-Jacketed RC Circular Bridge Columns. Journal of Structural Engineering, 120(8): 2358–2376.

De Zamacona Cervantes, G. (2019). Response of Idealized Structural Systems to Simulated M9 Cascadia Subduction Zone Earthquakes Considering Local Soil Conditions. M.S. Thesis, University of Washington, Seattle, WA.

DHS. (2019). Regional Resiliency Assessment Program (RRAP): Resiliency Assessment of Washington State Transportation Systems. Department of Homeland Security, Washington, D.C.

EERI (1989). Loma Prieta Earthquake, October 17.1989, Preliminary Reconnaissance Report. Report 89-03, Earthquake Engineering Research Institute.

EERI. (1994). Northridge Earthquake January 17, 1994, Preliminary Reconnaissance Report. Report 94-01, Earthquake Engineering Research Institute, Oakland, CA.

Frankel, A., Wirth, E., Marafi, N., Vidale, J., and Stephenson, W. (2018). Broadband Synthetic Seismograms for Magnitude 9 Earthquakes on the Cascadia Megathrust Based on 3D Simulations and Stochastic Synthetics, Part 1: Methodology and Overall Results. Bulletin of the Seismological Society of America, 108(5A): 2347–2369. DOI: 10.1785/0120180034.

Fung, G. G., Lebeau, R. J., Belvedere, J., and Goldschmidt, A. F. (1971). Field Investigation of Bridge Damage in the San Fernando Earthquake. Technical Report, California Department of Transportation.

Geyin, M., and Maurer, B.W. (2023). U.S. National VS30 Models and Maps Informed by Remote Sensing and Machine Learning. Seismological Research Letters. DOI: 10.1785/0220220181.

Gidaris, I., Padgett, J. E., Barbosa, A. R., and Chen, S. (2017). Multiple-Hazard Fragility and Restoration Models of Highway Bridges for Regional Risk and Resilience Assessment in the United States: State of the Art Review. Journal of Structural Engineering, 143(3). DOI: 10.1061/%28ASCE%29ST.1943-541X.0001672.

Kortum, Z., Liu, K.J., Eberhard, M., Berman, J., Marafi, N., and Maurer, B. (2021). Impacts of Cascadia Subduction Zone M9 Earthquakes on Bridges in Washington State: SDOF Idealized Bridges. WSDOT Final Report T1461, Task 74.

Lignos, D.G. and Krawinkler, H. (2012). Sidesway Collapse of Deteriorating Structural Systems under Seismic Excitations. The John A. Blume Earthquake Engineering Research Center, Stanford University, Report No. TB 177, Stanford, CA.

Mangalathu, S. (2017). Performance Based Grouping and Fragility Analysis of Box-Girder Bridges in California. Ph.D. Dissertation, Georgia Institute of Technology, Atlanta, GA.

Mangalathu, S., Jeon, J., and Jiquing, J. (2019). Skew Adjustment Factors for Fragilities of California Box-Girder Bridges Subjected to near-Fault and Far-Field Ground Motions. Journal of Bridge Engineering, 24(1). DOI: 10.1061/(ASCE)BE.1943-5592.0001338.

Marafi, N.A., Eberhard, M.O., Berman, J.W., Wirth, E.A., and Frankel, A.D. (2017). Effects of Deep Basins on Structural Collapse During Large Subduction Zone Earthquakes. Earthquake Spectra, 33(3): 963-997. DOI: 10.1193/071916EQS114M.

Mazzoni, S., McKenna, F., Scott, M.H., and Fenves, G.L. (2006). OpenSees Command Language Manual. OpenSees v1.7.3, University of California, Berkeley, USA.

McGuiness, S. (2021). Experimental Characterization of Steel Jacket Retrofitted Reinforced Concrete Bridge Column Behavior in Cascadia Subduction Zone Earthquakes. M.S. Thesis, Washington State University, Pullman, WA.

Motter, C.J, McGuiness, S., Bell, S., Quesnel, Z., and Phillips, A.R. (2023). Performance of Steel Jacket Retrofitted Reinforced Concrete Bridge Columns in Cascadia Subduction Zone Earthquakes. WSDOT Final Report.

National Institute of Standards and Technology (NIST) (1990). Performance of Structures during the Loma Prieta Earthquake of October 17, 1989. Special Publication 778, National Institute of Standards and Technology, Gaithersburg, MD.

Pacific Northwest Seismic Network. (2021). Cascadia Subduction Zone. https://pnsn.org/outreach/ earthquakesources/csz (May 31, 2021).

Priestley, M.J.N., Seible, F., Xiao, Y., and Verma, R. (1994a). Steel Jacket Retrofitting of Reinforced Concrete Bridge Columns for Enhanced Shear Strength – Part 1: Theoretical Considerations and Test Design. ACI Structural Journal, 91(4), 394–405.

Priestley, M.J.N., Seible, F., Xiao, Y., and Verma, R. (1994b). Steel Jacket Retrofitting of Reinforced Concrete Bridge Columns for Enhanced Shear Strength – Part 2: Test Results and Comparison with Theory. ACI Structural Journal, 91(5), 537–515.

Ramanathan, K.N. (2012). Next Generation Seismic Fragility Curves for California Bridges Incorporating the Evolution in Seismic Design Philosophy. Ph.D. Dissertation, Georgia Institute of Technology, Atlanta, GA.

Ranf, R.T. (2006). Performance Based Evaluation of Seismic Modeling Strategies for Bridges. Ph.D. Dissertation, University of Washington, Seattle, WA.

Ranf, R.T., Eberhard, M., and Malone, S. (2007). Post-Earthquake Prioritization of Bridge Inspections. Earthquake Spectra, 23(1): 131-146. DOI: 10.1193/1.2428313.

Shamsabadi, A. and Yan, L. (2008). Closed-Form Force-Displacement Backbone Curves for Bridge Abutment-Backfill Systems. Geotechnical Earthquake Engineering and Soil Dynamics Congress IV. DOI: 10.1061/40975(318)159.

WSDOT. (2020). Bridge Design Manual M 23-50.20. Washington State Department of Transportation, Bridge and Structures Office.

Zhu, M., McKenna, F., and Scott, M.H. (2018). OpenSeesPy: Python Library for the OpenSees Finite Element Framework. Volume 7, School of Civil and Construction Engineering, Oregon State University, Corvallis, OR.